We are IntechOpen, the world's leading publisher of Open Access books Built by scientists, for scientists

4,800
Open access books available

122,000
International authors and editors

135M
Downloads

Our authors are among the

154
Countries delivered to

TOP 1%
most cited scientists

12.2%
Contributors from top 500 universities

WEB OF SCIENCE™

Selection of our books indexed in the Book Citation Index in Web of Science™ Core Collection (BKCI)

Interested in publishing with us?
Contact book.department@intechopen.com

Numbers displayed above are based on latest data collected.
For more information visit www.intechopen.com

17

Diabetes Mechanisms, Detection and Complications Monitoring

Dhanjoo N. Ghista[1], U. Rajendra Acharya[2], Kamlakar D. Desai[3], Sarma Dittakavi[4], Adejuwon A. Adeneye[5] and Loh Kah Meng[6]
[1]*Department of Graduate and Continuing Education, Framingham State University, Framingham, Massachusetts,*
[2]*School of Engineering, Division of ECE, Ngee Ann Polytechnic,*
[3]*Mukesh Patel School of Technology Management & Engineering,*
[4]*Biomedical Engineering department, Osmania University,*
[5]*Department of Pharmacology, Faculty of Basic Medical Sciences, Lagos State University College of Medicine, Ikeja,*
Department of Pharmaceutical Sciences, College of Pharmacy, University of Kentucky, Kentucky,
[6]*VicWell Biomedical Private Limited,*
[1,5]*USA*
[2,6]*Singapore*
[3,4]*India*
[5]*Lagos State, Nigeria*

1. Introduction

Historically, the word *diabetes* was coined from the Greek word meaning a *siphon* by the 2nd century Greek physician, Aretus the Cappadocian. He used the word to connote a condition of passing water (urine) like a *siphon*. Later the Latin description *mellitus* meaning *sweetened or honey-like* was added. Put together, the term *diabetes mellitus* was literarily used to denote a disease condition which was associated with *the persistent passage of sweetened urine* (Krall & Braser, 1999).

In 1999, the World Health Organization described diabetes mellitus as a metabolic disorder of multiple aetiology characterized by chronic hyperglycaemia (the fasting blood glucose level equal or above 200 mg/dl taken at least twice, on different occasions) with disturbances of carbohydrate, fat and protein metabolism resulting from defects in insulin secretion, insulin action, or both. In other words, diabetes mellitus is a chronic disease with insidious onset in which the fasting blood glucose is persistently raised above the normal range values, the normal range being between 60 to 120 mg/dl of blood [Krall & Braser, 1999]. It occurs either because of a lack of insulin (the hormone responsible for glucose metabolism), or due to the presence of certain factors opposing the action of insulin on the body tissues that are involved in glucose metabolism, particularly, the liver and the skeletal muscles.

The consequence of insufficient insulin action is hyperglycaemia which may be associated with many associated metabolic abnormalities notably the development of hyperketonaemia

resulting from disordered protein metabolism, and derangements in fatty acid and lipids metabolism. If the fasting blood glucose lies between 100 to 130 mg/dl, it is referred to as *Prediabetes* which is associated with an increased tendency or potential of developing *frank* diabetes. A fasting blood glucose of 140 mg/dl or higher is consistent with either type of diabetes mellitus, particularly, when accompanied by classic symptoms of diabetes [Diabetes Control and Complication Trial Research Group, 1997].

2. Diabetes mechanisms

Defects in glucose metabolizing machinery (such as defective insulin secretion, insulin action due to de-expression of insulin receptors or insensitivity of expressed insulin receptors and glucose transporters, decreased peripheral glucose utilization and defective glucose metabolizing enzymes, *etc*.) and consistent efforts of the physiological system to correct the imbalance in glucose metabolism or maintain glucose homeostasis (such as increased insulin secretion, lipolysis, gluconeogenesis, glycogenolysis, *etc*.) place an over exertion on the endocrine system, resulting in hyperglycaemia. The persistent chronic exposure of pancreatic β-cells to the supraphysiological glucose concentrations (hyperglycaemia) results in non-physiological and potentially irreversible β-cell damage, a term known as glucose toxicity which is a gradual, time-related onset of irreversible lesion to pancreatic β-cellular components of insulin content and secretion.

Multiple biochemical pathways and cellular mechanisms for glucose toxicity have been identified and these include glucose autoxidation (resulting from oxidative stress in the presence of chronic hyperglycaemia), protein kinase C (PKC) activation, increased flux through the hexosamine biosynthesis pathway (HBP), formation of advanced glycation end-products (AGEs), altered polyol pathway flux and altered gene expression. However, all these pathways share in common the formation of highly reactive oxygen intermediates (ROIs) or reactive oxygen species (ROS) which in excess amount and on prolonged exposure induce chronic oxidative stress on the pancreatic β-cell population, which in turn causes defective insulin gene expression and insulin secretion as well as increase pancreatic β-cell death.

Hyperglycaemia leads to the production of ROS which modulates various biological functions by stimulating transduction signals, some of which are involved in the pathogenesis of diabetes mellitus. Thus, redox-sensitive signalling pathways have been shown to play a pivotal role in the development, progression, and damaging effect on β-cells population within the pancreatic islet of Langerhans. In the pancreatic tissues, as hyperglycaemia worsens, the redox-sensitive signalling pathways mediating insulin synthesis, storage and release from the pancreatic β-cells becomes compromised progressively. In addition, the oxidative stress induced by chronic hyperglycaemia promotes pancreatic β-cells apoptosis which ultimately resulting in an overt reduction in the insulin secreting pancreatic β-cells population. The hallmarks of these molecular events are pancreatic β-cells failure and hypoinsulinaemia, which constitute the major pathogenic factors in type 1 diabetes mellitus.

Similarly, chronic hyperglycaemia-induced oxidative stress (the presence of an excess amount of reactive oxygen intermediates, due to an imbalance between their formation and degradation as a result of chronic hyperglycaemia) has been considered a proximate cause and common pathogenic factor for tissue/systemic complications of diabetes such as endothelial cells (micro- and macro-angiopathies), nerve cells (neuropathy), proximal renal

epithelial cell (nephropathy), pancreatic β-cells (pancreatic β-cell failure) through lipid peroxidation and glycation mechanisms in these organs. Hyperglycaemia has been shown to result in glycation (a non-enzymatic conjugation of glucose to proteins leading to the formation of advanced glycation (glycosylation) end-products (AGEs) and tissue damage. Increased glycation and build-up of tissue AGEs have been implicated in the aetiology of diabetes mellitus, its complications and progression because they alter glucose metabolizing enzyme activity, decrease ligand binding, modify protein half-life and alter immunogenicity.

One mechanism by which the effects of glucose toxicity result in chronic hyperglycaemia are thought to be mediated is oxidative stress [Baynes, 1991; Evans *et al*., 2002], and hyperglycaemia is known to be one of the main causes of oxidative stress in type 2 diabetes mellitus [Bonnefont-Rousselot, 2002; Robertson *et al*., 2003]. Oxidative stress is a state of imbalance between free radical generation and mopping up.

Oxidative stress is known to play a pivotal role in the pathogenesis of insulin resistance which is itself is thought to be mediated via its contribution to glucose toxicity, particularly, in insulin target tissues including the pancreatic β-cells [Gleason *et al*., 2000; Fantus, 2004]. Tissues such as the mesangial cells (in the kidneys), retinal cells and pancreatic islets are least endowed with intrinsic antioxidant enzyme expression, including *superoxidases-1* and -*2*, *catalase* and *glutathione peroxidase* [Hayden & Tyagi, 2002; Robertson, 2004]. Prolonged exposure of pancreatic β-cell to hyperglycaemia, as in diabetes, results in decreased expression of the antioxidant gene *γ-glutamylcysteine ligase* (*γ-GCL*) and down-regulation of the rate-limiting enzyme for glutathione synthesis [Robertson, 2004]. The *γ-GCL* catalyses the rate-limiting step in the synthesis of γ-glutamyl cysteine from cysteine, which forms the substrate for the second enzyme regulating glutathione synthesis [Yoshida *et al*., 1995; Tanaka *et al*., 2002]. Reduced gluthathione plasma and tissue concentrations, as marked by elevated levels of ceruloplasmin, promote free radical generation, production of advanced glycation products (AGEs) and acute flunctuations in glucose concentrations.

In addition, oxidative stress promotes the onset and development of diabetes mellitus by directly decreasing insulin sensitivity and causing direct cytotoxicity to the pancreatic insulin-producing β-cells [Maiese *et al*., 2007]. The generated ROS penetrates through the cell membranes and reacts with the membrane phospholipids through the process of lipid peroxidation as well as reacts with the mitochondrial DNA to distrupt the mitochondrial respiratory machinery (mitochondrial electron transport) which is regulated by NADPH ubiquinone oxidoreductase and ubiquinone-cytochrome c reductase systems [Maiese *et al*., 2007].

Oxidative stress is known to depress the mitochondrial oxidoreductase and citrate synthase activities resulting in significant reductions in mitochondrial oxidative and phosphorylation activities as well as reduces the levels of mitochondrial proteins and mitochondrial DNA in adipocytes, particularly in type 2 diabetes mellitus (Petersen et al., 2003). Oxidative stress has been shown to trigger the opening of the mitochondrial membrane permeability transition pore which results in a significant depletion of mitochondrial NAD+ stores and subsequently apoptotic cell injury (Maiese et al., 2007). In the pancreatic tissues, these cellular events result in depletion of the β-cells population, insulin deficiency while in the skeletal muscle, it manifests as insulin resistance.

Oxidative stress is also known to modify a number of cellular signalling pathways that can results in insulin resistance. For example, a significant increase in muscle protein carbonyl

content (often used as a reliable biological marker of oxidative stress) and elevated levels of malondialdehyde and 4-hydrononenal (as reliable indicators of lipid peroxidation) have been implicated in the aetiology of insulin resistance diabetes mellitus [Haber *et al*., 2003].

3. Glucose-insulin regulatory system modeling and simulation of OGTT blood glucose concentration dynamics to obtain indices for diabetes risk and detection

This section deals with the bioengineering modelling of the glucose-insulin regulatory system and the OGTT blood glucose dynamics data, for more reliable detection of diabetes as well as designation of risk to diabetes.

The conventional way of diagnosing diabetes is based on designation of specific values of fasting plasma glucose equal or greater than 126 mg/dl (7.0 mmol/l), and (ii) 2-hour plasma glucose concentration equal or greater than 200 mg/dl (11.1 mmol/l) during OGTT. Instead of this rigid approach, we are proposing that for more reliable monitoring and diagnosis of diabetes, it is more relevant to mathematically characterise the trend of blood glucose concentration rise and decline after an oral intake of 75 g glucose load in OGTT. Hence, we provide the bioengineering analysis of the Glucose-insulin regulatory system and glucose response data, leading to the formulation of a novel nondimensional diabetes index for diagnosis of diabetic patients as well as of those who are at risk of becoming diabetic.

So, in this section, we present the Glucose-Insulin Regulatory System (GIRS) modeling in the form of governing differential equations, and converge to the equation representing blood glucose response to glucose infusion rate. This equation forms the basis of modeling of the Oral Glucose Tolerance Test (OGTT). We then demonstrate how this OGTT model equation's solutions can simulate the OGTT data, to evaluate the model parameters distinguishing diabetes subjects from normal subjects. The climax to this section is the formulation of the Non-dimensional Diabetes Index (DBI), involving combination of the model parameters into just "one number" by which we can reliably detect diabetes. In fact, by determining the range of values of DBI for a big patient population, we can even detect "patients at risk of being diabetic".

3.1 Differential equation model of the glucose-insulin system

With reference to the Blood Glucose-Insulin Control System (depicted in Fig. 1**)**, the corresponding first-order differential equations of the insulin and glucose regulatory sub-systems are given by equations (1) and (2) [Dittakavi et al., 2001].

$$x' = p - ax - \beta y \tag{1}$$

$$y' = q - \gamma x - \delta y \tag{2}$$

where x′ and y′ denote the first time-derivatives of x and y, x: insulin output, y: glucose output, p: insulin input, q: glucose input, for unit blood-glucose compartment volume (V). In these equations, the glucose-insulin model system parameters (regulatory coefficients) are $\alpha, \beta, \gamma, \delta$.

These coefficients, when multiplied by the blood-glucose compartment volume V (which is proportional to the body mass) denote, respectively,

- the sensitivity of insulinase activity to elevated insulin concentration (αV),

- the sensitivity of pancreatic insulin output to elevated glucose concentration (βV),
- the combined sensitivity of liver glycogen storage and tissue glucose utilization to elevated insulin concentration (γV), and
- the combined sensitivity of liver glycogen storage and tissue glucose utilisation to elevated glucose concentration (δV).

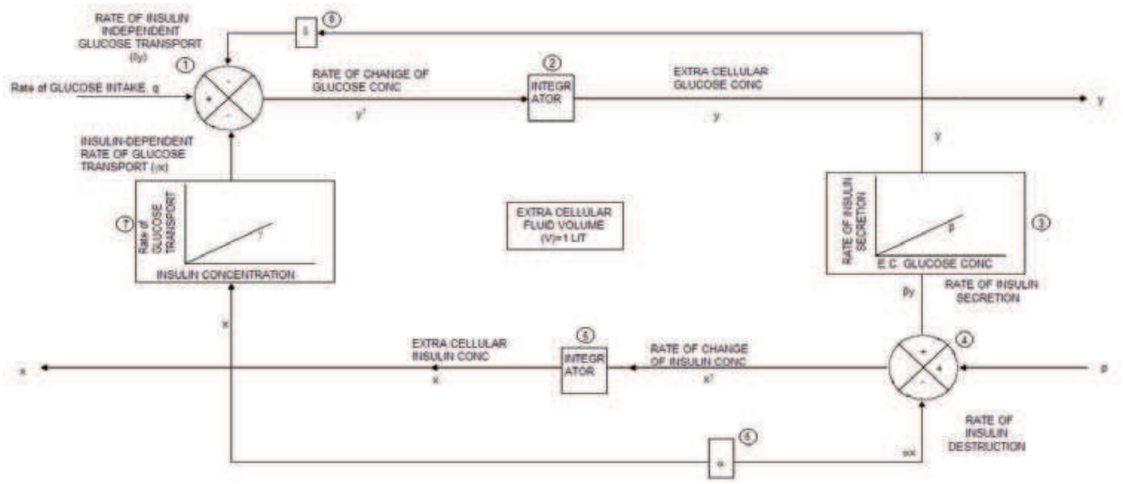

Fig. 1. Physiological model of the Blood Glucose Control system
(represented by equations 1 and 2).

From equations (1) and (2), the differential equation model in glucose concentration (y) for insulin infusion rate (p = 0) and glucose in flow rate (q), is obtained as

$$y'' + y'(\alpha + \beta) + y(\alpha\delta + \beta\gamma) = q' + \alpha q \tag{3}$$

where y' and y'' denote first and second time derivatives of y.
The transfer-function corresponding to Eqn. (3) is obtained by taking the Laplace transforms on both sides (assuming the initial conditions to be zero). Thereby, we obtain (for glucose response)

$$Y(s)/Q(s) = \frac{(s+\alpha)}{s^2 + s(\alpha+\delta) + (\alpha\delta + \beta\gamma)} = G(s) \tag{4}$$

3.2 Model analysis to simulate Oral Glucose Tolerance Test (OGTT)

The OGTT model-simulation response curve is considered to be the result of giving an impulse glucose dose (of 4 gm of glucose/liter of blood-pool volume) to the combined system consisting of GI tract and blood glucose concentration (BGCS). Now, we can put down the transfer-function (TF) of the gastro-intestinal (GI) tract to be 1/ (s + α), because the intestinal glucose-concentration variation is an exponential decay, and the exponential parameter value is close to that of the parameter α. When we multiply this GI tract TF [1/(s + α)] by the TF of the blood-pool glucose-metabolism given by Eqn. (4), and put Q(S) = 'G' gm of glucose per litre of blood-pool volume per hour, we get

$$Y(s) = G/\left\{s^2 + s(\alpha+\delta) + (\alpha\delta + \beta\gamma)\right\} \tag{5}$$

The corresponding governing differential equation is now:

$$y'' + 2Ay' + \omega_n^2 y = G\delta(t)$$

or

$$y'' + \lambda T_d y' + \lambda y = G\delta(t) \tag{6}$$

wherein ωn (= $\lambda^{1/2}$) is the natural frequency of the system, A is the attenuation or damping constant of the system, $\lambda = 2A/Td = \omega_n^2$, and $\omega = (\omega_n^2 - A^2)^{1/2}$ is the angular frequency of damped oscillation of the system.

The solution of Eq. (6), for an under-damped response (corresponding to that of normal subjects, represented by the lower curve in Fig. 2) is given by

$$y(t) = (G/\omega)e^{-At} \sin \omega t, \tag{7}$$

where in ω (or ω_d) = $(\omega_n^2 - A^2)^{1/2}$.

The solution for over-damped response (corresponding to that of diabetic subjects, represented by the upper curve in Fig 2) is given by:

$$y(t) = (G/\omega)e^{-At} \sinh \omega t \tag{8}$$

where in ω (or ω_d) = $(A^2 - \omega_n^2)^{1/2}$

The solution for a critically-damped response (in which $A = \omega_n$), which applies to subjects at risk of becoming diabetic (whose blood glucose response curve would lie between the two curves of normal and diabetic subjects), is given by:

$$y(t) = G\, t\, e^{-At}; \tag{9}$$

for $\omega_n^2 = A^2 = \lambda$, and derivative-time period $T_d = \frac{2A}{\lambda} = \frac{2A}{\omega_n^2}$

These solutions are employed to simulate the clinical data, and to therefore evaluate the model-system parameters A and ω (or λ and T_d), to not only differentially-diagnose diabetes subjects as well as sbut also to characterize resistance-to-insulin.

Now, we can employ equations (7) and (8) to simulate the OGTT data shown in Fig. 2 to obtain the value of parameters: (i) λ = 2.6hr−2, *Td* = 1.08 hr, for the normal subject, and (ii) λ =0.27hr−2 and *Td* = 6.08 hr, for the diabetic subject [Ghista, 2004].

We now formulate the Non-dimensional Diabetes Index (*DBI*), as

$$DBI = AT_d = \frac{2A^2}{\lambda} = \frac{2A^2}{\omega_n^2} \tag{10}$$

The value of *DBI* for the normal subject is 1.3, whereas for the diabetic subject it is 4.9. We have further found (in our initial clinical tests) that *DBI* for normal subjects is less than 1.6, while the *DBI* for diabetic patient is greater than 4.5. Hence a DBI value of 2-4 can suggest that the subject is at risk of becoming diabetic. This is a testimony of how well we have simulated the OGTT by our BME model and employed this DBI to diagnose diabetes.

$$y(t) = \frac{G}{\omega} e^{-ck} \sinh \omega t \qquad y(t) = \frac{G}{\omega} e^{-ck} \sinh \omega t$$

$$(AT_d = 4.9) \qquad (AT_d = 1.3)$$

$$(A = 0.808\ hr^{-1}, \lambda = 0.2657\ hr^{-2} \qquad (A = 1.4\ hr^{-1}, \lambda = 2.6\ hr^{-2}$$

$$T_d = 6.08\ hr, \qquad T_d = 1.08\ hr,$$

$$G = 2.9464\ gL^{-1}hr^{-1}) \qquad G = 1.04\ gL^{-1}hr^{-1})$$

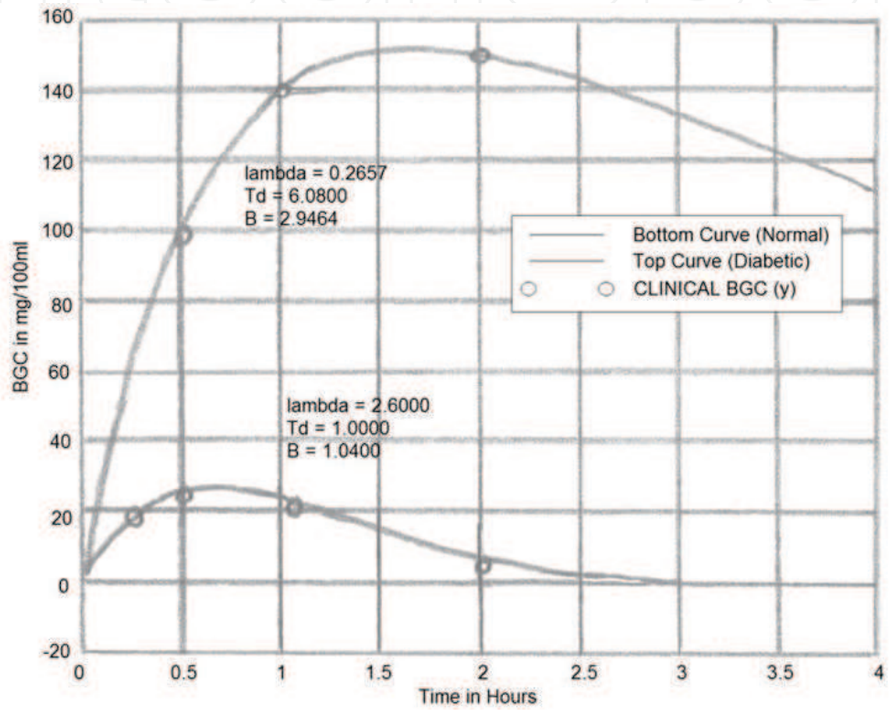

Fig. 2. OGTT Response Curve [Ghista, 2004], showing the glucose concentration responses of normal and diabetic subject.

4. Biomedical signal processing and image processing techniques for diabetes analysis

This section presents different signal and image processing methods that are used to evaluate the effect of diabetes on different organs.

4.1 Analysis of the heart rate variability signal

Heart rate variability (HRV) decreases in patients with diabetes [Acharya et al., 2006; Acharya et al., 2011b; Faust et al., 2011]. This variability can be analyzed in the time domain, frequency domain, and by using non-linear methods. Fig. 3 shows typical HRV signals of normal and diabetes subjects. Visually, it is difficult to notice the variability in these two signals. Hence, analysis in time domain and frequency domain with the use of non-linear methods is necessary. These methods are explained in this section.

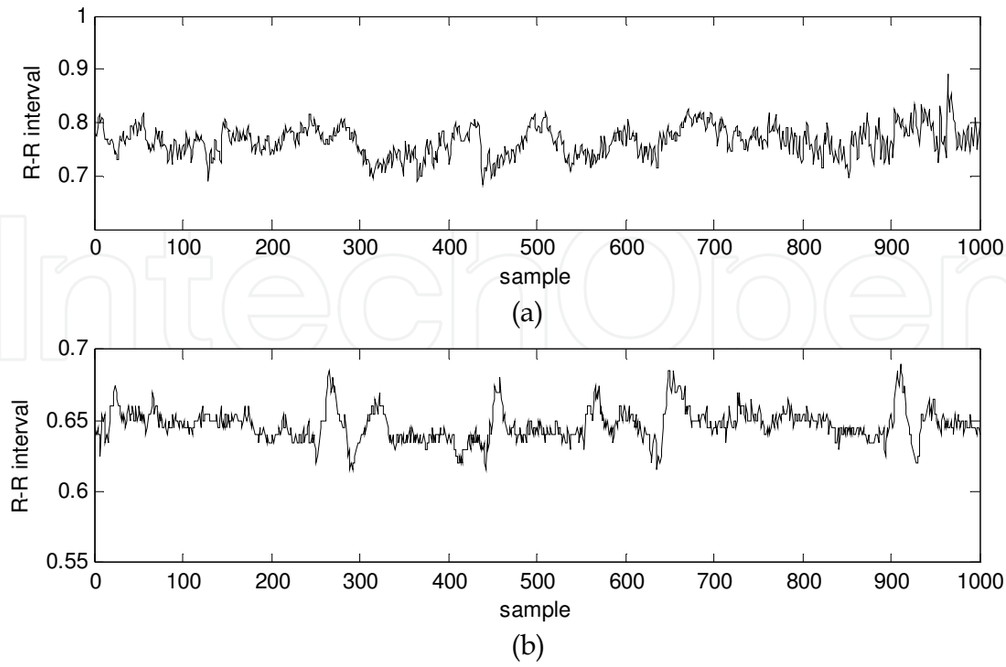

Fig. 3. Typical heart rate signals; (a) normal (b) diabetes.

4.1.1 Time domain analysis

The time-and frequency-domain measures of HRV were analyzed by the Task Force of the European Society of Cardiology [Task Force, 1996]. Several time domain parameters are calculated from the original R-R interval: mean R-R interval, standard deviation of the NN intervals (SDNN), standard deviation of differences between adjacent RR (NN) intervals (SDSD), Standard Error, or Standard Error of the Mean (SENN), which is an estimate of the standard deviation of the sampling distribution of means based on the data, number of successive difference of intervals which differ by more than 50 msec expressed as a percentage of the total number of ECG cycles analyzed (pNN50%).

The HRV triangular index (TINN) is the integral of the density distribution (i.e. the number of all NN intervals) divided by the maximum of the density distribution. Thus, six standard measures namely Mean RR, SDNN, SENN, SDSD, pNN50% and TINN were studied.

4.1.2 Frequency domain analysis

Spectral analysis of HRV signal results in three main components: high frequency (HF) component, low frequency (LF) component, and very low frequency (VLF) component [Task Force, 1996]. The influence of the vagus nerve in modulating the sinoatrial node is indicated by the HF component (0.15Hz -40Hz) of the spectrum. The LF component (0.04Hz-.155 Hz) indicates the sympathetic effects on the heart. The VLF component (0.003Hz -.04 Hz) explains many details of the heart, chemoreceptors, thermareceptors, and renin-angiotensin system [Task Force, 1996; Kamath et al., 1987; Van der Akker et al., 1983].

Fig. 4 shows a typical power spectral density (PSD) distribution of the heart rate signals obtained from a normal subject (Fig. 4-a) and a diabetes patient (Fig. 4-b). The beat to beat variation is greater in the normal heart rate signal compared to the diabetes heart rate signal. Hence, the power spectral density is more predominant in HF in the normal subject[Faust et al., 2011].

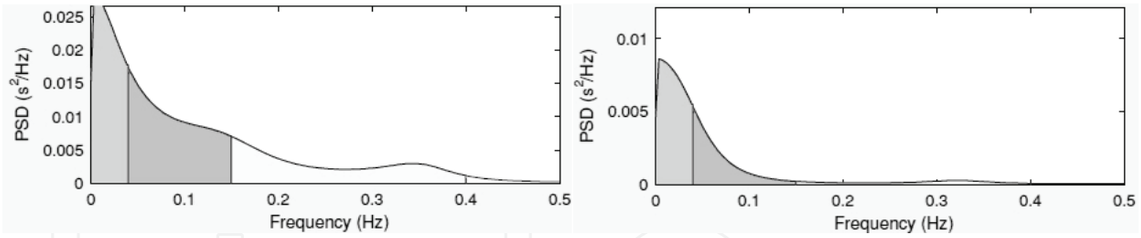

(a) (b)

Fig. 4. Typical power spectral density of heart rate signal (a) normal (b) diabetes subject. The PSD of normal heart rate signal has LF, HF components. The diabetic heart rate signal, however, does not have HF components due to lower variability in the heart rate signal [Acharya et al., 2011b].

4.1.3 Non-linear parametric analysis of heart rate signals

Various non-linear parameters can be used to analyze the diabetes heart rate signals. They are Approximate Entropy (ApEn), Correlation Dimension (CD), Largest Lyapunov Exponent (LLE), The Hurst exponent (H), Recurrence plot (RP), and Fractal Dimension (FD).

The Approximate Entropy *ApEn* measures regularity of the time series. The method proposed by Pincus et al can be used to evaluate the ApEn [Pincus, 1991]. For the data points $x(1), x(2),..., x(N)$, with an embedding dimension *m*, the ApEn or $APEN$ is given by:

$$APEN(m, r, N) = \frac{1}{N-m+1}\sum_{i=1}^{N-m+1}\log C_i^m(r) - \frac{1}{N-m}\sum_{i=1}^{N-m}\log C_i^{m+1}(r) \quad (11)$$

where $C_i^m(r) = \frac{1}{N-m+1}\sum_{j=1}^{N-m+1}\Theta\left(r - \left\|\mathbf{x}_i - \mathbf{x}_j\right\|\right)$ is the correlation integral. For this study, m is set to 2, and r is chosen as 0.15 times the standard deviation of the original data sequence, and N is the total number of data points.

The *Correlation dimension (CD)* is a quantitative measure of the informational complexity of the heart rate signal [Grassberger, 1983]. Some unique ranges of CD for different cardiac diseases have been proposed by Acharya et al. [2007]. The formula for CD involves the correlation function *C*(*r*), which is the probability that two arbitrary points on the orbit are closer together than *r*. This is done by calculating the separation between every pair of *N* data points and sorting them into bins of width d*r* proportionate to *r*. The correlation dimension can be calculated by using the distances between each pair of points in the set of N number of points, $a(i, j) = \left|X_i - X_j\right|$

$$C(r) = \frac{1}{N^2} \times \left(Number\ of\ pairs\ of\ (i, j)\ with\ a(i, j) < r\right) \quad (12)$$

Correlation dimension (CD) is given by:

$$CD = \lim_{r \to 0} \frac{\log\left(C(r)\right)}{\log(r)} \quad (13)$$

The Largest Lyapunov Exponent (LLE) measures the predictability of the system and determines sensitivity of the system to initial conditions [Rosenstien et al., 1993]. A positive LLE indicates chaos. The LLE is estimated by using a least squares fit to "average "line, and is given by:

$$y(n) = \frac{1}{\Delta t}\langle \ln\left(d_i(n)\right)\rangle \tag{14}$$

where $d_i(n)$ is the distance between i^{th} phase-space point and its nearest neighbor at n^{th} time step, and $\langle . \rangle$ denotes the average overall phase space points.

The Hurst Exponent (HE) indicates the self-similarity and correlation properties of heart rate signal. The *HE* has been defined and proposed by Dangel et al [Dangel et al., 1999]. Unique range of H values has been proposed by Acharya et al, for various cardiac states [Acharya et al., 2007].

$$\mathrm{H} = \log(\mathrm{R}/\mathrm{S})/\log(\mathrm{T}) \tag{15}$$

where T is the duration of the sample of data and R/S is the corresponding value of rescaled range. An *HE* value of 0.5 indicates the presence of a random walk, *HE* < 0.5 depicts anti persistence, and *HE* > 0.5 indicates the persistence in the signal.

The *Recurrence plot (RP)* can be used to unearth the non-stationarity in the heart rate signals [Acharya et al., 2006], and was originally introduced by Eckmann et al. [Eckmann et al., 1987].

A Fractal is a set of points which, when looked at smaller scales, looks similar to the whole group [Madelbrot, 1983]. The Fractal Dimension (FD) determines the complexity of the time series. FD has been used in heart rate analysis to recognise and differentiate specific states of physiologic functions [Acharya et al., 2007].

The heart rate signal is a non-linear and non-stationary signal. The hidden intricacies of the signal can be easily extracted using non-linear analysis methods. The heart rate variation is more random in normal subjects as compared to the diabetes subjects. Hence, most of these non-linear parameters may show distinct values for normal and diabetes subjects. These clinically significant non-linear parameters can be fed into the classifiers as features for automatic classification. Moreover, these non-linear parameters can be combined in the form of an integrated index [Ghista, 2004; 2009a; 2009b]. Such an index may have unique range of values for normal and diabetes classes. Hence, one can diagnose normal and diabetes subjects by just using one index value without the need for automatic classifiers.

4.2 Image processing of digital fundus images in diabetic retinopathy

Diabetic retinopathy is an important complication of diabetes. As the diabetes retinopathy progresses, the number of blood vessels varies, and the exudates appear in the advanced DR stages [Yun et al., 2008; Acharya et al., 2011a]. Different image processing techniques have been used to extract blood vessels and exudates in DR subjects, and these techniques are explained in this section. Moreover, techniques for plantar pressure images analysis, which have proved to be useful in detecting diabetic neuropathy conditions, are also been presented in this section.

4.2.1 Retinal blood vessels detection

The detailed steps involved in the blood vessel detection are shown in Fig. 5 [Nayak et al., 2008; Acharya et al., 2011a; Acharya et al. 2009; Acharya et al., 2011b]. The green

component of the RGB (Red, Green Blue) blood vessel image is considered for this study. The border of the image is obtained by applying an edge detection algorithm on the inverted green component of the image. Morphological operation is performed by using a disk shaped structuring element (SE) for blood vessels detection. Adaptive histogram equalization is then performed on these images to enhance the image, and subsequently, morphological opening operation is performed using a ball structuring element. Thresholding is carried out on the resulting image followed by the median filtering to obtain the boundary of the image. The small holes are then filled and the boundary is removed. Finally, the image with only blood vessels is obtained (Fig. 7) [Acharya et al., 2011b]. It can be seen from Fig. 7(a) that the number of blood vessels is different in the normal and the proliferative diabetes retinopathy (PDR) classes.

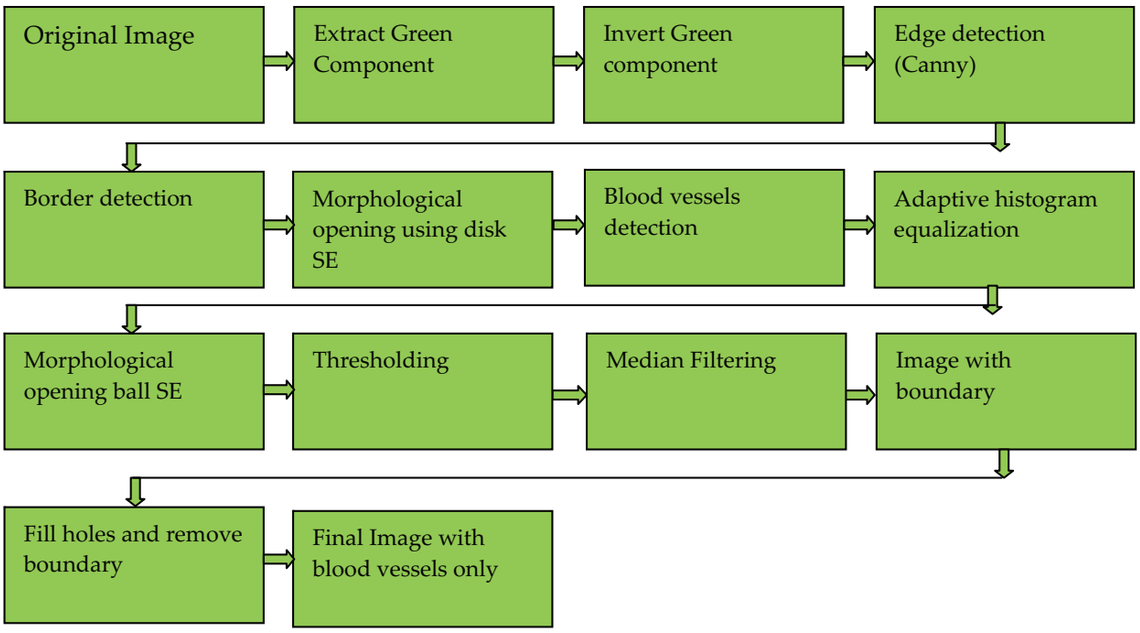

Fig. 5. The block diagram for detecting retinal blood vessels.

4.2.2 Exudates detection in digital fundus images

Fig. 6 shows the block diagram of the exudates extraction in digital fundus images [Acharya et al., 2008; Nayak et al., 2008; Acharya et al., 2011a; Acharya et al., 2011b]. The green component of the original image is extracted and subjected to the morphological closing operation by using octagonal shaped structuring element. Then, the resulting image is subjected to thresholding, and morphological closing operation is carried out by using disk shaped SE.

The edges are detected by using the Canny method. Subsequently, an 80x80 region of interest (ROI) is considered to remove the optic disc, and then the border of the image is also removed. Finally, by performing morphological erosion operation with disk shaped SE of size 3, the final image with only exudates is obtained (Fig. 7) [Acharya et al., 2011b]. It can be seen from the Fig. 7(b) that there are no exudates in the normal image, while the PDR image has exudates.

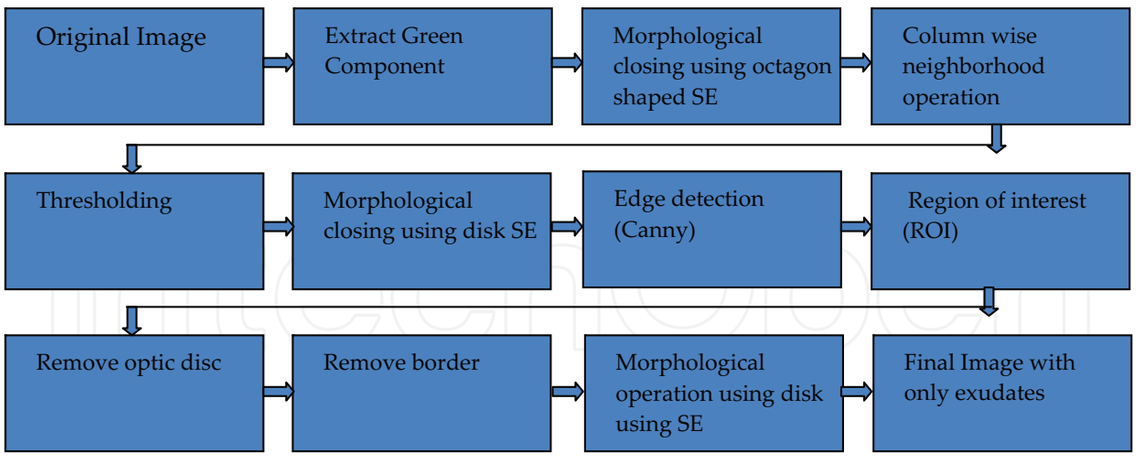

Fig. 6. The block diagram for detecting exudates in digital fundus images.

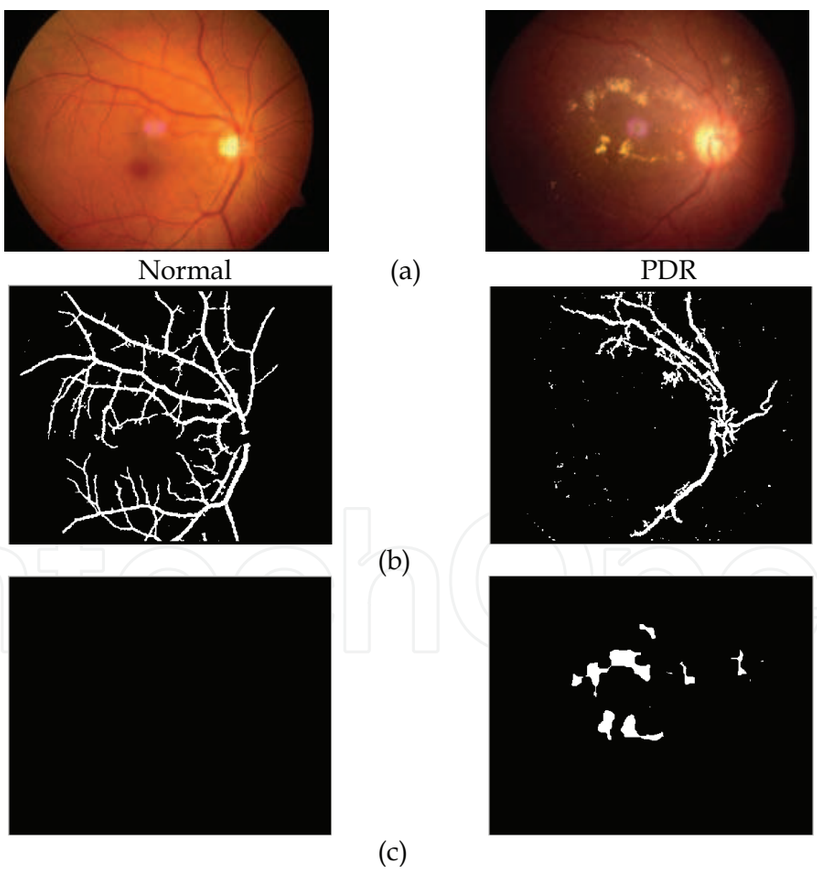

Fig. 7. Results of blood vessel detection and exudate detection from normal and PDR images. (a) Original normal and PDR images (b) Results of blood vessel detection (c) Results of exudate detection. The number of blood vessels are different for normal and PDR images, and exudates are absent in the normal fundus image.

4.3 Plantar pressure distribution image analysis

Fig. 8 shows the plantar pressure distribution images of normal subjects, and subjects with diabetes type II without and with neuropathy. It can be seen from the figure that the pressure distribution is different for normal, diabetes without and with neuropathy subjects [Acharya et al., 2008; Acharya et al., 2011b]. This difference can be further analyzed using Fourier transform and discrete wavelet transform (DWT).

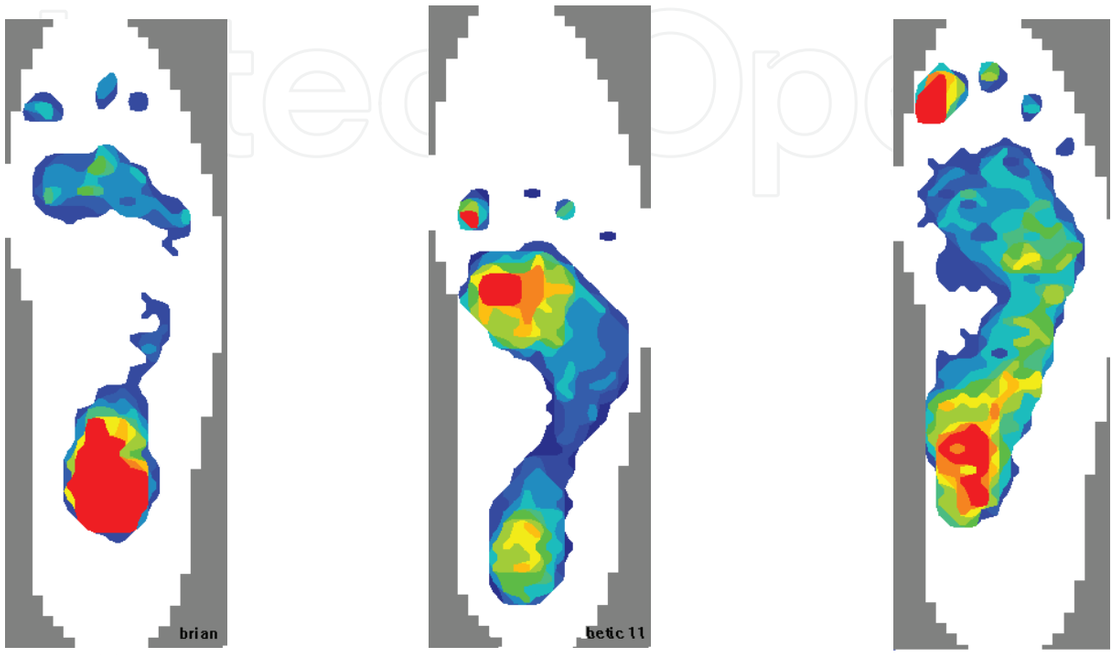

(a) (b) (c)

Fig. 8. Static pedobarograph images of (a) the normal foot, (b) a diabetic foot with neuropathy, and (c) a diabetic foot without neuropathy.

The important feature used to diagnose the normal, diabetes type II with and without neuropathy classes is the power ratio (PR) that is obtained using the Fourier transform [Rahman et al., 2006]. This method is clearly explained below.

Fourier domain analysis: The Fourier spectrum *F(u,v)* of each region of the image can be obtained by using the below equation (16) [Cavanagh et al., 1991]. In this equation, *M* and *N* represent the numbers of rows and columns of the image. The power ratio (*PR*) is the ratio of the high frequency power (*HFP*) to the total power (*TP*). The Fourier spectrum is given by

$$F(u,v)=\frac{1}{MN}\sum_{x=0}^{M-1}\sum_{y=0}^{N-1}f(x,y).e^{-j2\Pi\left(\frac{ux}{M}+\frac{vy}{N}\right)} \tag{16}$$

where x, y, u *and* v are the variables.

$F(0,0)$ is the DC component of the image in the frequency domain and is the sum of all the pixels of an image in spatial domain [Cavanagh et al., 1991]. The *total power (TP)* of the image is given by

$$TP=\left\{\sum\sum|F(u,v)|^2\right\}-|F(0,0)|^2 \tag{17}$$

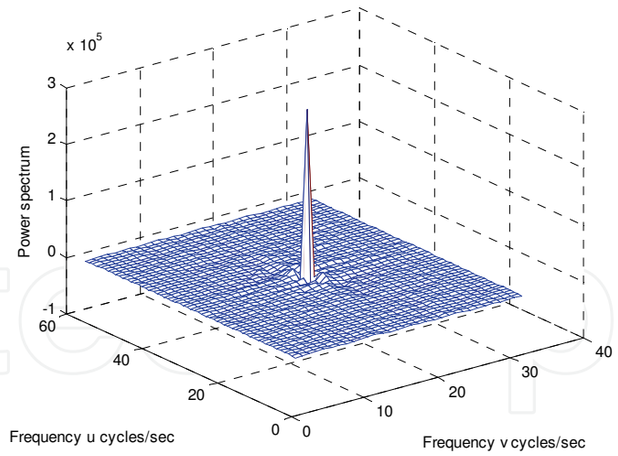

(a)

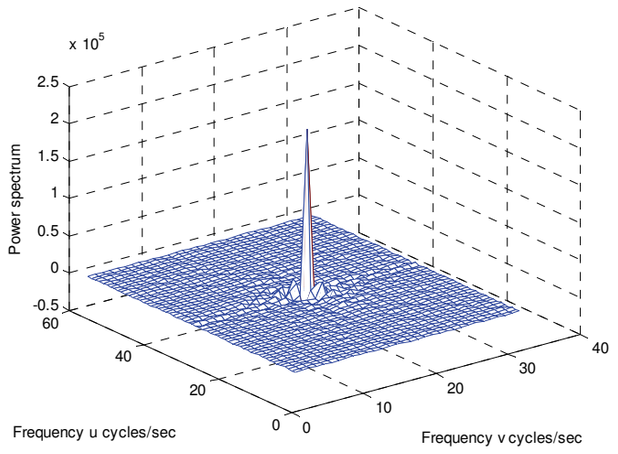

(b)

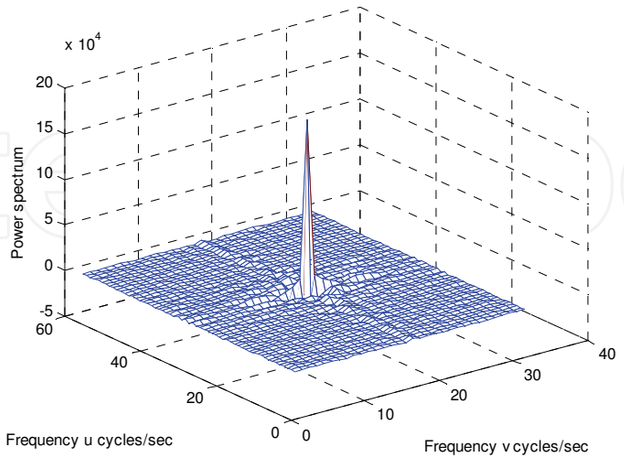

(c)

Fig. 9. Typical power spectra after deleting the DC component from region 6 of the left foot for (a) normal subject (b) diabetes subject without neuropathy (c) diabetes subject with neuropathy[Acharya et al., 2011b].

The low frequency and high frequency components are separated by S_o, which is given by

$$S_o = \begin{cases} \frac{M}{4} & if\ M \le N \\ \frac{N}{4} & if\ M < N \end{cases} \tag{18}$$

$$LFP = \left\{ \sum_{S(u,v)=0}^{S_o} |F(u,v)|^2 \right\} - |F(0,0)|^2 \tag{19}$$

$$HFP = TP - LFP \tag{20}$$

$$PR = \left(\frac{HFP}{TP} \right) x100 \tag{21}$$

where *LFP, HFP*, and *PR,* denote the low frequency power, high frequency power, and the power ratio, respectively.

Fig. 9 shows the typical power spectra obtained for a normal subject, having diabetes without neuropathy, and subject having diabetes with neuropathy. It is a 3D figure, with u and v frequencies corresponding to row and column. The Y-axis indicates the power. The power spectrum of normal class has a peak in the centre and very small peaks around it. In the case of diabetes without neuropathy, the adjacent peaks are slightly larger; in the case of diabetes with neuropathy, there are dominating peaks on four sides. These plots are unique and depict variation of power spectrum. The PR values extracted from various regions of the plantar image are shown in Table 1[Acharya et al., 2011b].

Type	Control subjects (CS)	Diabetic control (DC)	Neuropathic (N)	p-value
Region 1	12.80 ± 3.49	9.562 ± 2.25	17.657 ± 3.27	<0.0001
Region 2	11.865 ± 2.13	9.678 ± 2.58	14.453 ± 2.31	<0.0001
Region 5	13.769 ± 3.31	9.512 ± 2.530	14.542 ± 2.69	<0.0001
Region 6	10.179 ± 2.09	9.697 ± 1.23	12.35 ± 2.19	<0.0001
Region 7	9.28 ± 6.03	8.67 ± 3.30	11.56 ± 1.45	<0.0001

Table 1. Power ratio values for the various regions of the plantar pressure images obtained from the three classes.

The PR is the ratio of HF power to the total power. This value is higher for diabetes subjects with neuropathy when compared to the normal and diabetes without neuropathy subjects for regions 1, 2, 5, 6, and 7 (Table 1). These ranges are unique and clinically significant ($p<0.0001$). These PR features can be used to diagnose the three classes automatically using classifiers.

Likewise, DWT coefficients have also been used to identify the normal, diabetes type II with and without neuropathy classes [Acharya et al., 2008; Acharya et al., 2011b].

5. Diabetic autonomic neuropathy diagnosis from HRV power spectrum plots

The RR interval files are processed to get HRV and HRVPS [Desai, K.D et al., 2011]. The sampling frequency used to get HRV form RR file is 2Hz. The power spectrum plots depict power in $(BPM)^2$ versus Frequency (in Hertz). The auto regression statistics gives display of the following parameters:
Power under Low frequency range: frequency range from 000 to 0.04Hz
Power under Mid frequency range: frequency range from 0.04 to 0.15Hz
Power under High frequency range: frequency range from 0.15 to 0.40Hz
Sympatho/Vagal balance ratio: ratio of mid to high frequency powers
The Sympatho-Vagal ratio is found in the different frequency characteristics of the parasympathetic and sympathetic influences on heart rate. The HRVPS plots (for the supine, standing and deep breathing modes) are plotted with time-scale up to 150 seconds and heart rate scale in the range of 40 bpm to 140 bpm.

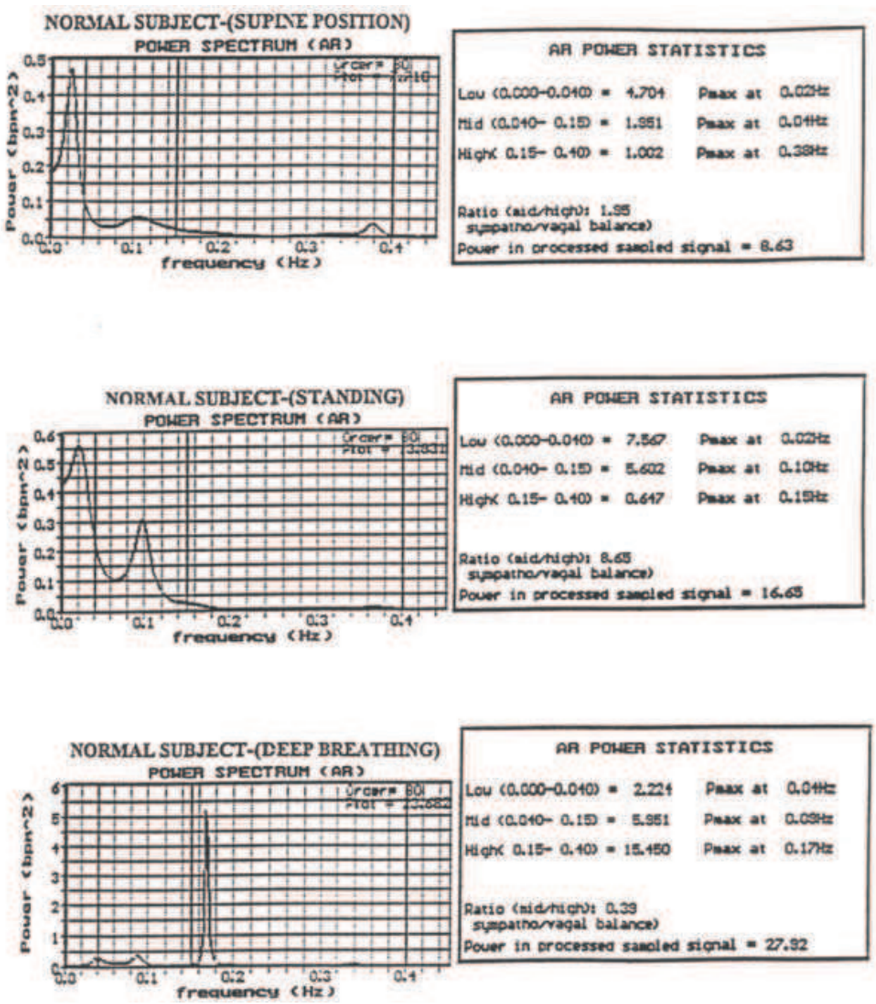

Fig. 10. HRVPS plots of a normal subject in supine, standing and deep breathing modes. The power statistics on the right side show the power in low, medium and high frequency bands. There is an increase in the mid frequency power in standing position and in high frequency power in deep breathing mode.

Figure 10 displays the HRVPS of a typical normal subject in supine, standing and deep breathing modes. In this figure, the power statistics show the power in low, medium and high frequency bands. It can be noted that there is an increase in the mid-frequency power in standing position and in the high-frequency power in deep breathing mode. Figure 11 depicts the HRVPS plot of a typical diabetic subject in supine, standing and deep-breathing modes. Now, it can be seen that there is a decrease in mid-frequency power and in high-frequency power in deep-breathing mode compared to corresponding power levels of a normal subject (in Figure 10) [Desai, K.D et al., 2011].

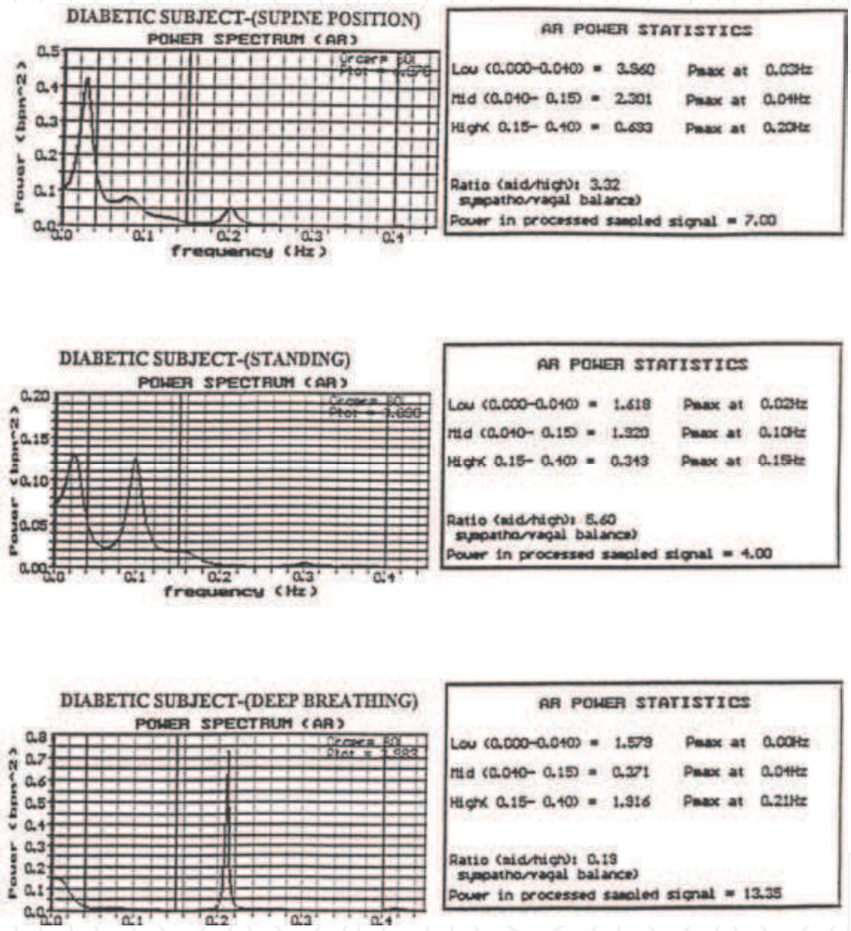

Fig. 11. HRVPS plots of a diabetic subject in supine, standing and deep breathing modes. The power statistics on the right side show the power in low, medium and high frequency bands. There is a decrease in the mid frequency power in standing position and in high frequency power in deep breathing mode compared to corresponding power levels of normal subject as shown in Fig 10a[Desai, K.D et al., 2011].

5.1 Diagnostic indices (based on HRVPS)

The analysis of HRV power spectra is commonly focused on the power in different frequency bands. In particular, the power in the high-frequency range reflects the fast parasympathetic never activity [Fallen et al., 1985], and the power in the mid-frequency range reflects both parasympathetic and sympathetic never activity [Akselrod, S., et al., 1981].

The ratio of the mid-frequency range power to the high-frequency range power is sometimes used as a relative index of the sympatho/vagal balance [Bianchi et al., 1990]. The high frequency range power ratio between supine and standing position is used as a parasympathetic index [Fallen et al., 1985]. The same ratio is used to study sympathetic function in standing position in the mid frequency range [Fallen et al., 1985]. Sympathetic vasomotor nerve function is quantified by the baro receptor oscillation frequency (i.e., the mid-peak frequency) in the HRVPS [Kamath et al., 1987].

In our study, autonomic function indices are defined in terms of spectral power indices and HRV period (or frequency) shift indices. The mid and high-frequency ranges are considered for defining indices. The diagnostic indices are based on parameters measured from the HRVPS. The values of diagnostic indices for the three groups of subjects have shown significant difference and can provide rational basis for selecting prognostic therapy before a diabetic patient develops cardiac arrhythmic complications.

The **diagnosis indices** are defined as follows:

$$I_1 = \text{Relative sympathetic} - \text{to} - \text{vagal balance index} = P_2 / P3\,, \tag{22}$$

where

(P_2)=area under HRVPS spectral plot between 0.04 Hz and 0.15 Hz

(P3)=area under HRVPS spectral plot between 0.15 and 0.4 Hz.

$$I_2 = \text{Orthostatic Stress Index } = (\text{P2sta} - \text{P2sup}) / \text{P2sup}\,, \tag{23}$$

where

(P2)=area under HRVPS spectral plot between 0.04 Hz and 0.15 Hz, and subscripts 'sta' and 'sup' refer to standing supine positions.

$$I_3 = \text{Sympatho} - \text{Vagal Integrity Index} = \sum(\text{Hrmax} - \text{Hrmin}) / \text{n}\,, \tag{24}$$

where

HRmax = Local maximum heart rate (beats per minute) during one breathing cycle.

HRmin = Local minimum heart rate (beats per minute) prior to local maximum in the same breathing cycle.

n=number of breathing cycles.

$$I_{4std} = \text{Sympathetic HRV} - \text{Spectral Frequency Shift Index}(\text{standing}) = (F2_{std} - 0.1) / 0.1, \tag{25}$$

where F_2 = Frequency of the Baroreceptor reflex peak

$$I_{5sup} = \text{Sympathetic HRV} - \text{Spectral Frequency Shift Index}(\text{supine}) = (F2_{supine} - 0.1) / 0.1 \tag{26}$$

$$I_6 = \text{Respiratory Stress Index} = (P_{3db} - P_{3supine})\,, \tag{27}$$

where

$$(P_{2supine}) = \text{area under HRVPS spectral plot frequency 0.04 Hz and 0.15 Hz in supine position}\,. \tag{28}$$

$$\left(P_{3db}\right)=\text{area under HRVPS spectral plot between frequency 0.15 Hz and 0.4 Hz in deep breathing .} \tag{29}$$

$$\left(P_{3supine}\right)=\text{area under HRVPS spectral plot between frequency 0.15 Hz and 0.4 Hz in supine position .} \tag{30}$$

The following Table 2 shows the calculated indices, for a sample normal subject, obtained from the HRVPS parameters.

Autonomic	Index Formula	Index Value
Relative Sympathetic-to-Vagal Balance Index	$I_1 = P_2/P_3$	$I_{1(sup)} = 2.06$ $I_{1(st)} = 7.82$ $I_{1(db)} = 0.32$
Orthostatic Stress Index	$I_2 = (P_{2sta} - P_{2sup})/P_{2sup}$	$I_2 = 1.64$
Sympatho-Vagal Integrity	$I_3 = \sum (HR_{max} - HR_{min}) / n$	$I_3 = 6.62$
HRV-Freq-Shift Index (standing)	$I_4 = (F_{2std} - 0.1) / 0.1$	$I_4 = -0.05$
HRV-Freq-Shift Index (supine)	$I_{5sup} = (F_{2supine} - 0.1) / 0.1$	$I_5 = -0.10$
Respirator Stress Index	$I_6 = (P_{3db} - P_{3supine}) / P_{3supine}$	$I_6 = 16.70$

Table 2. Computed Indices for a typical normal subject.

In this Table 2, $I_{1(sp)} = P_2/P_3$ (equation 22) in supine position; $I_{2(st)} = P_2/P_3$ (equation 22) in standing position; $I_{2(db)} = P_2/P_3$ (equation 22) in deep – breathing mode.
Now, diagnosis based on six indices makes it somewhat difficult to track in a patient as regards how much each index varies from its normal value, for making an appropriate diagnosis. So now we will adopt the novel approach, as in Ghista [Ghsta, 2004; 2009a], of formulating an index by combining the parameters in such a way that the index values are distinctly different for normal subjects, diabetics, and diabetics with ischemic heart disease. Hence, we are proposing that, from a diagnostic and classification viewpoint, it would be more convenient to formulate a DAN Integrated Index (DAN-IID) [Desai, K.D et al., 2011], as :

$$\text{DAN}-\text{IID} = \left[\left(\text{I1,st}\right)+\left(\text{I1,db}\right)+\left(\text{I2}\right)+\left(\text{I3}\right)+\left(\text{I6}\right)\right]-\left[\left(\text{I4}\right)+\left(\text{I5}\right)\right] \tag{31}$$

5.2 Results and analysis: HRVPS of normal subjects, diabetic subjects, and diabetic subjects with ischemic heart disease

The instantaneous heart rate average (IHRav), average of difference between maximum and minimum heart rate over a cycle (ΔHrav), power and frequency measurements (P,F) measured from HRVPS are determined. There from the diagnostic indices are computed (as per equation 22-27).

Descriptive Statistics of Indices of the Three Groups

The computed indices for the three categories of subjects are displayed in the following Tables
Table 3 for normal subject group.
Table 4 for diabetic subject group.

Table 5 for IHF subject group.
Then, using the values in Tables (2), (3) and (4), the mean and standard deviation values of three groups are calculated and presented in the Table 6.

Name	I_{1sp}(N)	$I_{1,st}$(N)	$I_{1,db}$(N)	I_2(N)	I_3(N)	I_4(N)	I_5(N)	I_6(N)	DAN-IID
Ahamidm	2.08	14.57	0.51	3.78	3.26	-0.1	-0.07	16.26	38.55
Awmeah	2.07	7.83	0.33	1.64	6.62	-0.05	-0.1	16.7	33.27
Fahmia	1.88	2.67	0.36	2.04	8.56	0.13	-0.1	17.81	31.41
Fatimah	0.47	7.46	0.84	1.08	4.9	-0.57	0.07	0.24	15.02
Gitakr	1.93	3.93	2.49	2.66	9.51	0.03	-0.07	2.8	21.43
Indvai	1.63	8.25	0.26	2.01	3.86	-0.4	-0.07	16.14	30.85
Kploga	1.4	2.31	0.3	2.32	7.66	-0.12	0.5	10.67	22.88
Mattarh	1.21	9.17	2.02	2.2	3.59	-0.52	-0.07	1.53	19.1
Mohdsae	3.09	1.47	0.3	-0.65	4.43	-0.08	0.13	1.81	7.31
Mohsed	5.78	9.95	0.75	1.36	6.63	-0.02	0.1	21.87	40.48
Ramial	8.95	3.53	0.18	0.92	11.73	0.3	0.1	8.69	24.65
Sekarm	2.15	5.19	0.25	0.02	3.29	-0.05	0.3	9.88	18.38
Average	2.72 ±2.36	6.36 ±3.87	0.71 ±0.75	1.61 ±1.19	6.17 ±2.76	-0.12 ±0.25	6.0E-02 ±0.18	10.36 ±7.45	25.277 ±9.88

Table 3. Results of Indices for normal subject group.

Name	I_{1sp}(D)	$I_{1,st}$(D)	$I_{1,db}$(D)	I_2(D)	I_3(D)	I_4(D)	I_5(D)	I_6(D)	DAN-IID
Ahmedn	3.54	7.09	0.19	-0.06	2.83	-0.08	-0.57	1.88	12.58
Altmoh	2.07	4.95	0.31	-0.32	2.47	-0.57	-0.57	5.40	13.95
Aminaha	1.34	2.11	0.70	-0.28	2.94	-0.57	-0.57	1.08	7.69
Bakmh	4.25	2.45	0.52	-0.35	1.66	-0.57	-0.57	25.00	30.42
Elmamol	0.51	0.49	0.44	-0.41	2.25	-0.57	-0.57	-0.47	3.44
Fikria	3.57	12.72	0.16	0.78	1.51	-0.57	-0.57	16.89	33.2
Ghyarh	3.78	7.75	1.56	-0.36	2.81	-0.52	-0.57	0.20	13.05
Humoya	3.58	3.78	0.68	2.80	3.68	-0.35	-0.57	4.59	16.45
Kmilmo	2.84	5.30	0.59	0.11	2.38	-0.30	-0.57	1.15	10.4
Krshpr	0.85	0.59	0.13	-0.36	1.86	-0.57	-0.57	20.42	23.78
Kurubrl	1.55	1.74	3.08	0.03	1.44	-0.57	-0.57	3.78	11.21
Mahabs	1.54	5.78	1.06	0.51	6.91	-0.57	-0.57	1.28	16.68
Mohdosb	4.39	1.92	0.32	-0.76	2.01	0.03	0.01	1.32	4.77
Mohikat	2.41	0.55	0.29	-0.29	1.87	-0.57	-0.23	13.25	16.47
Muisdr	0.86	1.08	3.30	-0.30	2.98	-0.10	-0.57	0.34	8.07
Nasah	2.59	26.95	1.19	1.83	2.09	-0.32	0.57	0.44	32.25
Naya	0.75	3.51	3.92	-0.71	1.36	-0.57	-0.57	-0.58	8.64
Salmm	0.35	1.89	0.54	-0.30	0.78	-0.57	-0.57	-0.59	3.43
Average	2.26 ±1.36	5.03 ±6.31	1.05 ±1.17	8.66E-02±0.9	2.43 ±1.32	0.43 ±0.2	-.455 ±0.29	5.29 ±7.94	14.804 ±9.43

Table 4. Results of Indices for diabetic subject group.

Name	$I_{1,sp}$(H)	$I_{1,st}$(H)	$I_{1,db}$(H)	I_2(H)	I_3(H)	I_4(H)	I_5(H)	I_6(H)	DAN-IID
Aminase	0.45	0.74	0.99	-0.81	1.45	-0.57	-0.57	1.74	5.25
Hamamak	6.22	1.73	0.52	-0.63	1.77	-0.57	-0.57	13.10	17.63
Mayara	2.03	3.80	1.00	0.52	2.90	-0.23	-0.08	5.53	14.06
Mdshr	1.33	1.05	0.11	0.21	3.41	-0.57	-0.05	9.62	15.02
Mohmust	2.14	2.45	1.34	0.10	2.22	-0.57	-0.28	0.69	7.63
Omarsh	2.95	2.60	0.22	-0.49	2.17	-0.20	-0.02	1.79	6.51
Shamsa	0.66	1.10	2.57	-0.16	1.78	-0.57	-0.57	0.25	6.68
Tamebr	2.79	7.10	2.09	2.50	1.58	-0.57	-0.15	9.60	23.59
Average	2.32 ±1.82	2.57 ±2.09	1.1 ±0.87	0.155 ±1.05	2.16 ±0.68	-0.48 ±0.16	-.28 ±0.24	5.29 ±4.93	12.046 ±10.85

Table 5. Results of Indices for ischemic heart disease subject group.

Index	Normal (N)		Diabetic (D)		Diabetic + IHD (H)	
	Mean	Sd	Mean	Sd	Mean	Sd
I_1 (supine)	2.719	2.357	2.266	1.356	2.32	1.821
I_1 (standing)	6.361	3.864	5.036	6.312	0.155	1.49
I_1 (deep breathing)	0.715	0.755	1.053	1.166	1.107	0.869
I_2 (orthostatic stress)	1.614	1.185	0.085	0.908	0.155	1.049
I_3 (sympatho-vagal integrity)	6.195	2.736	2.435	1.323	2.16	0.681
I_4 (sym HRVPS freq shift by standing)	-0.121	0.257	-0.439	0.203	-0.481	0.165
I_{5sup} (sym HRVPS freq shift in sup)	0.06	0.185	-0.519	0.152	-0.286	0.248
I_6 (resp stress index)	10.366	7.447	5.261	7.969	5.29	4.92
DAN-IID	25.277	9.88	14.804	9.43	12.046	6.57

Table 6. Descriptive Statistics of indices of the three groups.

Diagnostically significant indices

In order to demonstrate the effectiveness of the diagnostic indices (I_1 to I_6) to distinguish the three groups, the diagnostically significant indices are calculated using Mann Whitney Wilicoxon Rank test (Non-Parametric Tests), and the p values(<0.05)are tabulated in Table 7 below[Desai, K.D et al., 2011].

Index	Significance Between Two Groups	P-value(<0.05)
I_1 (standing)	N & H	0.0109
I_2	N & H	0.0253
I_3	N & H	0.0004
I_4	N & H	0.0025
I_5	N & H	0.0083
I_2	N & D	0.0020
I_3	N & D	0.0000
I_4	N & D	0.0015
I_5	N & D	0.0000
I_6	N & D	0.0422
I_5	H & D	0.0105

Table 7. Diagnostically Significant Indices.

5.3 Physiological relevance of the computed indices

The computed indices reflect the sympatho-vagal interactions that modulate cardiovascular function. The low-frequency component (in the 0.04Hz to 0.15Hz range) of the HRV power spectrum (F_2 peak) is an indicator of sympathetic modulation, and the high frequency component (in the 0.15Hz to 0.4Hz range) in the HRV power spectrum (F_3 peak) is a marker of vagal modulation.

The index I_1 (= P_2/P_3) represents relative sympathetic-to-vagal balance, I_1 is found to be reduced to a very low value, from 6.361 to 0.155 in standing position in the case of diabetics with ischemic heart disease. This indicates that diabetics with ischemic heart disease are not able to withstand orthostatic stress or load. Patients recovering from an acute myocardial infarction can be expected to have an increased I1 index during early convalescence, and a return to a normal value by 6 to 12 months

The orthostatic stress index I_2 shows significant reduction from a normal value of 1.614 to 0.085 in diabetics, and, to 0.155 in diabetics with ischemic heart disease. A similar trend is noted for **the sympatho-vagal integrity index I_3,** showing reduction in the index value from a normal value of 6.19 to 2.43 in the case of diabetics, and to 2.16 in diabetics with ischemic heart disease. This is indicative of damage to the sympathetic and parasympathetic systems controlling the SA node pacing activity

The sympathetic HRVRS frequency-shift Index in standing position (I_{4sd}) and Sympathetic HRVPS frequency-shift Index in supine position (I_{5sup}) are found to be decreased in diabetics as well as in diabetics with ischemic heart disease patients, compared to the normal subject group. This is indicative of the increased delay (of more than 10 seconds) in case of diabetics as well as diabetics with ischemic heart disease, due to demyelination of their nervous control system controlling the heart rate.

The Respiratory Stress Index I_6 denotes the effectiveness of vagal control on heart rate variation, and is found to be considerably reduced from a normal value of 10.36 to 5.26 in diabetics, and to 5.29 in diabetics with ischemic heart disease.

Thus the indices derived from the HRV power spectrum represent non-invasive signatures of the balance between sympathetic and parasympathetic components of the autonomic nervous system. These indices are shown to characterize diabetic autonomic neuropathy state, and to hence distinguish diabetics and diabetics with ischemic heart disease.

Integrated index composed of power-spectral indices

We have shown how well the HRVPS indices differentiate normal subjects from diabetics and diabetics with ischemic heart disease.

We now compute the values of this integrated Index (DAN-IID) for normal subjects (in Table 3), diabetic subjects (in Table 4), and diabetic patients with ischemic heart disease (in Table 5) . From these Index values, we compute its mean values and standard deviations, for normals, diabetics, and diabetics with ischemic heart disease (IHD). These values are tabulated in Table 6. It can be clearly seen, from this Table 6, that our integrated Index can be employed to effectively differentiate and diagnose diabetic subjects and diabetics with IHD. The Index can also be employed to assess the efficacy of diabetic medication and insulin administration.

We next make a distribution plot of this Integrated Index for normals, diabetics, and diabetics with IHD, in Figure 12. This plot graphically illustrates how well this integrated Index separates normal subjects, diabetic patients, and diabetic patients with ischemic heart disease[Desai, K.D et al., 2011].

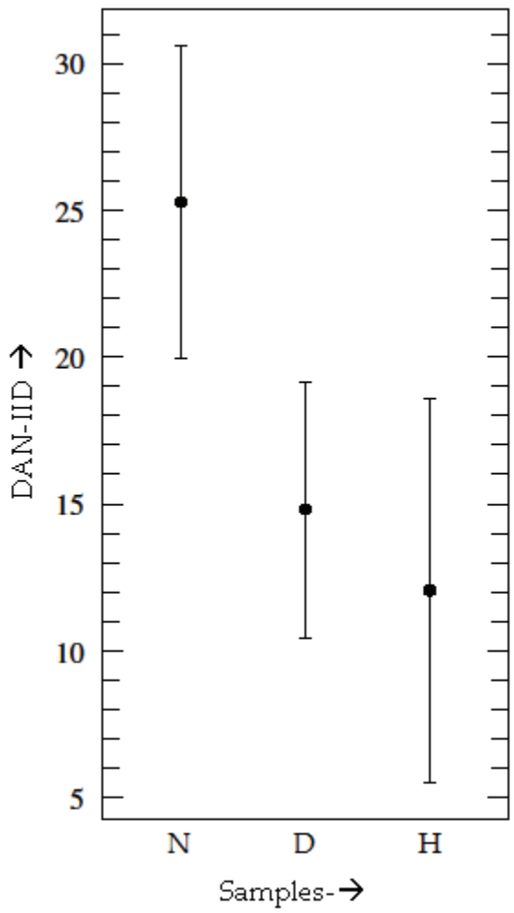

Fig. 12. Variation of DAN-IID for (N) normal subjects, (D) diabetic patients, and (H) diabetics with IHD. It can be noted that this DAN-IID clearly separates diabetics and diabetics with IHD from normal subjects.

6. Activity-based dynamic insulin infusion system

In section 3, we have introduced the glucose-insulin regulatory system and applied it to model the OGTT. We came up with our novel DBI, by means of which we can even detect supposedly normal subjects who are at risk of becoming diabetic. Now, we continue on the trail of this glucose-insulin regulatory system, by presenting its application to illustrate how for a diabetic patient the glucose level keeps going up after meal, and how it is regulated by automated infusion of insulin.

Herein, we demonstrate the operation of a Glucose activity-based Dynamic Insulin infusion (or release) system. The current insulin infusion systems are based on the diabetic patient's known activities history, in order to estimate the required insulin amount. These techniques do not allow the patients to deviate too much from their normal daily activities [Naylor et al., 1996]. Hence, our approach focuses on regular sampling of the diabetic patients' blood glucose concentration through a sensor, to compute the required amount of insulin to be released into the blood stream.

The amount of insulin infused to bring the blood glucose concentration down is regulated by a Closed-loop PD (Proportional-Derivative) Control system algorithm (Fig. 13). The closed loop system continuously monitors the blood glucose concentration at 0.5 h interval. Once the system detects that the blood glucose concentration exceeds a predetermined threshold e.g. 120mg/dl [International Diabetes Federation], the system is alarmed and 'calculates' the amount of insulin required [Loh, 2004] to bring the blood glucose concentration below the threshold.

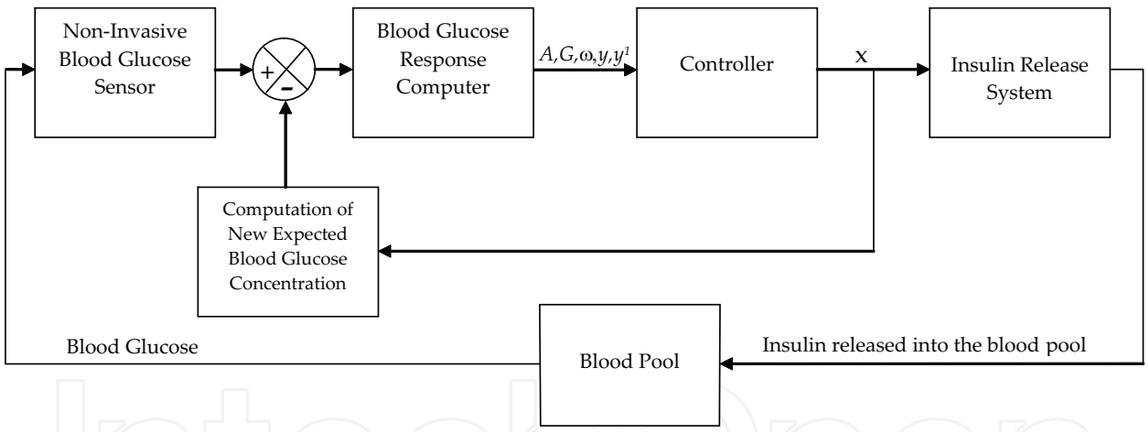

Fig. 13. Block diagram of the Glucose Regulating Insulin Release (GRIR) system: The glucose sensor monitors the existing blood glucose level. The error between the glucose sensor level and the computed expected blood glucose concentration is fed into the Closed-loop PD (Proportional-Derivative) Control system, and its algorithm computes the amount of insulin (x) to be released. Accordingly, the required amount of insulin is released into the blood. This now readjusts the blood glucose level, which is again monitored by the sensor.

Then, Fig. 14 shows the results of the application of the Insulin Infusion Release system of Fig 13. The diabetic subject D18's unaided glucose clinical data is fed into the system. On the Y axis, we have plotted blood-glucose concentration above the patient's glucose concentration of 120 mg/dl (or 1.2 g/l) at time 0 after meal. The insulin is released at 0.5 hour, 1 hour and 1.5 hours after meal. In figure 16, it is seen, how following insulin infusion, the blood glucose comes down. Once the blood glucose concentration drops below the threshold, the controller will stop releasing insulin into the blood stream.

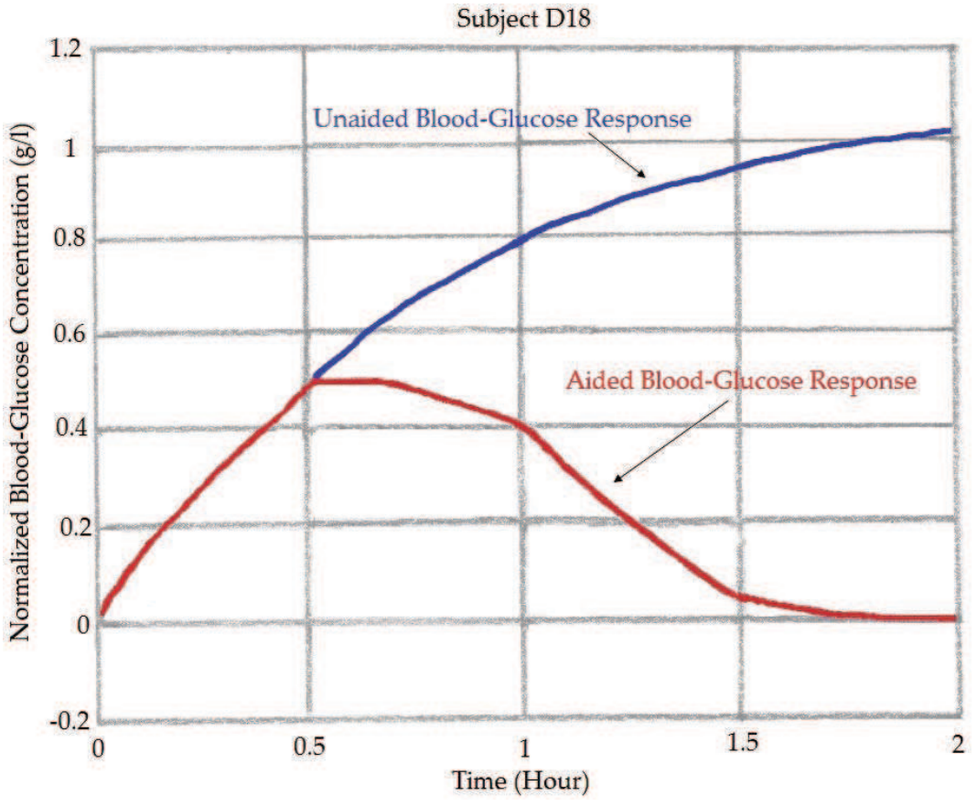

Fig. 14. The subject's unaided blood glucose concentration at time 0 is above 120mg/dl. The system is alarmed and samples the blood glucose concentration at 0.5h (170 mg/dl). The system sends a bolus of insulin 10mU/dl into the blood stream. The system keeps monitoring the resulting blood glucose concentration at 1.0h and 1.5 hour intervals, and infuses computed insulin bolus into the blood stream to bring the blood glucose concentration below the threshold value.

Thus, we have demonstrated the capability of the activity based adaptive dynamic real-time insulin release system. This system is able to protect the users from hyperglycemia.

7. Conclusion

This chapter is framed to provide useful insights into: (i) the mechanisms of diabetes; (ii) how the bioengineering analysis of the glucose regulatory system can be employed to diagnose diabetic patients and subjects at risk of becoming diabetic, based on an integrated index composed of parameters of the governing differential equation to simulate blood glucose concentration data of OGTT; (iii) parameters of time-and frequency-domain measures of HRV can be employed to differentiate diabetic subjects from normal subjects; (iii) processing of retinal digital fundus images to characterize retinopathy, and analysis of plantar pressure distribution images of normal subjects, and subjects with diabetes type II without and with neuropathy, (iv) diagnosis of diabetic autonomic neuropathy by means of a novel intregrated index composed of parameters of heartrate variability power-spectrum plots; (v) how we can apply the glucose-insulin regulatory system to illustrate how for a diabetic patient the glucose level keeps going up after meal, and how it is can be regulated by automated infusion of insulin.

8. Acknowledgments

Authors thank Journal of Mechanics in Biology and Medicine (published by World Scintific Publishing Co. Pte Ltd) for giving permission reproduce the portions of materials from their published papers, (i) U Rajendra Acharya, Jasper Tong, Vinitha Sree, Chua Kuang Chua, Tan Peck Ha, Dhanjoo N Ghista, Subhagata Chattopadhyay, Kwan-Hoong Ng, Jasjit S Suri, "Computer-Based Identification of Type 2 Diabetic Subjects With and Without Neuropathy using Dynamic Planter Pressure and Principal Component Analysis", Journal of Medical Systems, 2011 (In Press: DOI: 10.1007/s10916-011-9715-0); (ii) Desai, K.D, Dhanjoo N. Ghista, Issam Jaha El Mugamex, U Rajendra Acharya, Michael Towsey, Sultan Abdul Ali, Mohammed Saeed, M. Amin Fikri, *"Diabetic Autonomic Neuropathy Detection By Heart-Rate Variability Power-Spectral Analysis"*, Journal of Mechanics in Medicine and Biology, 2011 (In Press); (iii) Dhanjoo N Ghista, "Nondimensional Physiological Indices for Medical Assessment", Journal of Mechanics in Medicine and Biology, 9(4), 2009, 643-669.

9. References

Acharya, U.R.; Lim, C.M.; Ng, E.Y.K.; Chee, C. & Tamura, T. (2009). Computer-based detection of diabetes retinopathy stages using digital fundus images. *Proc Instn Mech Engrs. J Eng Med Part H,* Volume 223, No. 5, pp. 545-553.

Acharya, U.R.; Tan, P.H.; Subramaniam, T.; Tamura, T.; Chua, K.C.; Goh, S.C.E.; Lim, C.M.; Goh, S.Y.D.; Chung, K.R.C.& Law, C.(2008). Automated identification of diabetic type 2 subjects with and without neuropathy using wavelet transform on pedobarograph. *J Med Syst*, Volume 32, No. 1, pp.21-29.

Acharya, U.R.; Joseph, P.K.; Kannathal, N.; Lim, C.M. & Suri, J.S.(2006). Heart rate variability: A Review, *Med Biol Eng Comput*, Volume 44, No. 12, pp. 1031-1051.

Acharya, U.R.; Suri, J.S.; Spaan, J.A.E. & Krishnan, S.M.(2007). Advances in Cardiac Signal Processing. Springer Verlang GmbH. Berlin, Heidelberg.

Acharya, U.R.; Rahman, M.A.; Aziz, Z.; Tan, P.H.; Ng, E.Y.K. & Yu, W. (2008). Computer-based identification of plantar pressure in type 2 diabetes subjects with and without neuropathy. *Journal of Mechanics in Medicine and Biology,* Volume 8, No.3, pp. 363-375.

Acharya, U.R.; Faust, O.; Dua, S.; Hong, S.J.; Yang, T.S.; Lai, P.S. & Choo, K. (2011a). Computer-based diagnosis of diabetes retinopathy stages using digital fundus images. Dua S, Acharya UR, Ng EYK (Eds.), 'Computational image modeling of human eye with applications', *World Scientific Publishing Company*.

Acharya, U.R.; Ghista, D.N.; Nergui, M.; Chattopadhyay, S.; Ng, E.Y.K.; Sree, V.S.; Tong, J.W.K.; Tan, J.H.; Loh, K.M.& Suri, J.S. (2011b). Diabetes Mellitus: Enquiry into its Medical aspects and Bioengineering of its Monitoring and Regulation. *Journal of Mechanics in Medicine and Biology* (In Press).

Akselrod, S., et al (1981), Power spectrum analysis of heart rate fluctuation: A quantitative probe of beat-to-beat cardiovascular control, Science, Vol. 213, 10, pp. 220-222 .

Baynes, J.W. (1991). Role of oxidase stress in development of complications in diabetes (Review). *Diabetes*, Vol. 40, No. 4, pp. 405-412.

Bianchi, A., et al (1990) Spectral analysis of heart rate variability signal and respiration in diabetic subjects, Medical & Biological Engineering & Computing, Vol. 28, pp. 205-211.

Bonnefont-Rousselot, D. (2002). Glucose and reactive oxygen species. *Current Opinion in Clinical Nutrition and Metabolic Care*, Vol. 5, No. 5, pp. 561-568.

Cavanagh, P.R.; Sims, D.S.& Sanders, Jr. L.J. (1991). Body mass is a poor predictor of peak plantar pressure in diabetic men. *Diabetes Care*, Volume 14, pp.750-755.

Dangel, S.; Meier, P.F.; Moser, H.R.; Plibersek, S. & Shen, Y.(1999). Time series analysis of sleep EEG. *Computer Assisted Physics,* pp. 93-95.

Desai, K. D.; Ghista, D.N.; Mugamex, I. J. El.; Acharya, U.R.; Towsey, M.; Ali, S.A.; Saeed, M., Fikri, M. A. (2011). Diabetic Autonomic Neuropathy Detection By Heart-Rate Variability Power-Spectral Analysis*, Journal of Mechanics in Medicine and Biology*, 2011 (In Press);

Dittakavi, S.S. & Ghista, D.N.(2001). Glucose tolerance tests modeling & patient simulation for diagnosis. *J Mech Med Biol,* Volume 1, No.2, pp.193-223.

Eckmann, J.P.; Kamphorst, S.O. & Ruelle, D.(1987). Recurrence plots of dynamical systems. *Europhys Lett,*Volume 4, pp. 973-977.

Evans, J.L.; Golfine, I.D.; Maddux, B.A. & Grodsky, G.M. (2002). Oxidative stress and stress-activated signalling pathways: a unifying hypothesis of type 2 diabetes. *Endocrine Reviews*, Vol. 23, No. 5, pp. 599-622.

Fallen, E.L., Nandogopal, D., Connonlly, S., and Ghista, D.N. (1987) "How reproducible is the power spectrum of heart rate variability in health subjects?", Proceedings of International Symposium on Neural and Cardiovascular Mechanisms, Bologna, Italy May, 1985.

Fantus, G. (2011). Diabetes, glucose toxicity. http://www.endotext.org/diabetes/diabetes12new/diabetes12.htm

Faust, O.; Acharya, U.R.; Molinari, F.; Chattopadhyay, S. & Tamura, T. (2011). Linear and Non-Linear Analysis of Cardiac Health in Diabetic Subjects. *Biomedical Signal Processing and Control*, 2011

Ghista, D.N.(2004). Physiological systems' numbers in medical diagnosis and hospital cost effective operation. *J Mech Med Biol*., Volume 4, No. 4,pp. 401–418.

Ghista, D.N.(2009a). Nondimensional physiological indices for medical assessment. *J Mech Med Biol.,* Volume 9, No. 4, pp. 643-669.

Ghista, D.N. (2009b). Applied Biomedical Engineering Mechanics. *CRC Press*.

Gleason, C.E.; Gonzalez, M.; Harmon, J.S. & Robertson, R.P. (2000). Determinants of glucose toxicity and its reversibility in the pancreatic islet beta-cell line, HIT-T15. *American Journal of Physiology, Endocrinology and Metabolism*, Vol. 279, No. 5, pp. E997-E1002.

Grassberger, P. & Procassia, I.(1983). Measuring the strangeness of strange attractors. *Physica,* Volume D9, pp.189-208.

Haber, C.A.; Lam, T.K.; Yu, Z.; Gupta, N.; Goh, T.; Bogdanovic, E.; Giacca, A. & Fantus, I.G. (2003). N-acetylcysteine and taurine prevent hyperglycaemia-induced insulin resistance *in vivo*: possible role of oxidative stress. *American Journal of Physiology: Endocrinology and Metabolism*, Vol. 285, No. 4, pp. E744-E753.

Hayden, M.R. & Tyagi, S.C. (2002). Islet redox stress: the manifold toxicities of of insulin resistance, metabolic syndrome and amylin derived islet amyloid in type 2 diabetes mellitus. *Journal of Pharmacology*, Vol. 3, No. 4, pp. 86-108.

International Diabetes Federation. Website: http://www.idf.org/2000, last accessed in Dec 2010.

Kamath, M.V.; Ghista, D.N.; Fallen, E.L.; Fitchett, D.; Miller, D. & McKelvie, R.(1987). Heart rate variability power spectrogram as potential noninvasive signature of cardiac regulatory system response, mechanisms, and disorders. *Heart Vessels*, Volume 3, pp.33-41.

Krall, L.P. & Beaser, R.S. (1989). *Joslin Diabetes Manual* (12th edition), Lippincott Williams and Wilkins, ISBN 978012111200, London (United Kingdom).

Loh, K.C. (2004). Pharmacology of Oral Anti-hyperglycaemic Agents & Insulin (Invited Article). *Singapore Family Physician*, Volume 30, pp.16-20.

Maiese, K.; Chong, Z.Z. & Shang, Y.C. (2007). Mechanistic insights into diabetes mellitus and oxidative stress. *Current Medicinal Chemistry*, Vol. 16, No. 16, pp. 1729-1738.

Mandelbrot, B.B.(1983). Geometry of Nature. Freeman San Francisco.

Nayak, J.; Bhat, P.S.; Acharya, U.R.; Lim, C.M. & Gupta, M.(2008). Automated identification of different stages of diabetic retinopathy using digital fundus images. *J Med Syst*, Volume 32, No. 2, pp. 107-115.

Naylor, C.D.; Sermer, M.; Chen, E. & Sykora, K.(1996). Cesarean delivery in relation to birth weight and gestational glucose tolerance: pathophysiology or practice style? Toronto Tri-Hospital Gestational Diabetes Investigators. *JAMA,* Volume 275, pp.1165.

Petersen, K.F.; Befroy, D.; Dufour, S.; Dziura, J.; Ariyan, C.; Rothman, D.L.; DiPietro, L.; Cline, G.W. & Shulman, G.I. (2003). Mitochondrial dysfunction in the elderly: possible role in insulin resistance. *Science*, Vol. 300, No. 5622, pp. 1140-1142.

Pincus, S.M.(1991). Approximate entropy as a measure of system complexity. *Proc National Academic Science,* Volume 88, pp.2297-2301.

Rahman, M.A.; Aziz, Z.; Acharya, U.R.; Tan, P.H.; Natarajan, K.; Ng, E.Y.K.; Law, C.; Subramaniam, T. & Shuen, W.Y.(2006). Analysis of plantar pressure in diabetic Type 2 subjects with and without neuropathy. *Innov Technol Biol Med*, Volume 27, No. 2, pp.46-55.

Robertson, R.P. (2004). Chronic oxidative stress as central mechanism for glucose toxicity in pancreatic islet beta cells in diabetes. *Journal of Biological Chemistry*, Vol. 279, No. 41, pp. 42351-42354.

Robertson, R.P.; Harmon, J.; Tran, P.O.; Tanaka, Y. & Takahashi, H. (2003). Glucose toxicity in β-cells: Type 2 diabetes, good radicals gone bad, and glutathione connection. *Diabetes*, Vol. 52, No. 3, pp. 581-587.

Rosenstien, M.; Colins, J.J. & De Luca, C.J.(1993). A practical method for calculating largest Lyapunov exponents from small data sets. *Physica D*, Volume 65, pp. 117-134.

Tanaka, Y.; Tran, P.O.; Harmon, J. & Robertson, R.P. (2002). A role for glutathione peroxidase in protecting pancreatic beta cells against oxidative stress in a model of glucose toxicity. *Proceedings of National Academy of Science (USA)*, Vol. 99, No.19, pp. 12363-12368.

Task Force of the European Society of Cardiology and North American Society of Pacing and electrophysiology.(1996). Heart Rate Variability: Standards of measurement, physiological interpretation and clinical use. *Eur Heart J,* Volume 17, pp.354-381.

Van der Akker, T.J.; Koeleman, A.S.M.; Hogenhuis, L.A. & Rompelman, G.(1983). Heart-rate variability and blood pressure oscillations in diabetics with autonomic neuropathy. *Automedica*, Volume 4, pp.201-208.

Yoshida, K.; Hirokawa, J.; Tagami, S.; Kawakami, Y.; Urata, Y. & Kondo, T. (1995). Weakened cellular scavenging activity against oxidative stress in diabetes mellitus: regulation of glutathione synthesis and efflux. *Diabetologia*, Vol. 38, No. 2, pp. 201-210.

Yun, W.L.; Acharya, U.R.; Venkatesh, Y.V.; Chee, C., Lim C.M. & Ng, E.Y.K.(2008). Identification of different stages of diabetic retinopathy using retinal optical images. *Information Sciences*, Volume 178, No. 1, pp.106-121.

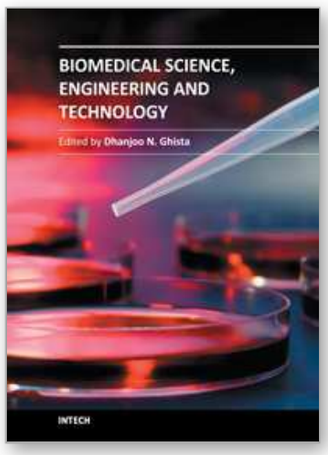

Biomedical Science, Engineering and Technology

Edited by Prof. Dhanjoo N. Ghista

ISBN 978-953-307-471-9
Hard cover, 902 pages
Publisher InTech
Published online 20, January, 2012
Published in print edition January, 2012

This innovative book integrates the disciplines of biomedical science, biomedical engineering, biotechnology, physiological engineering, and hospital management technology. Herein, Biomedical science covers topics on disease pathways, models and treatment mechanisms, and the roles of red palm oil and phytomedicinal plants in reducing HIV and diabetes complications by enhancing antioxidant activity. Biomedical engineering coves topics of biomaterials (biodegradable polymers and magnetic nanomaterials), coronary stents, contact lenses, modelling of flows through tubes of varying cross-section, heart rate variability analysis of diabetic neuropathy, and EEG analysis in brain function assessment. Biotechnology covers the topics of hydrophobic interaction chromatography, protein scaffolds engineering, liposomes for construction of vaccines, induced pluripotent stem cells to fix genetic diseases by regenerative approaches, polymeric drug conjugates for improving the efficacy of anticancer drugs, and genetic modification of animals for agricultural use. Physiological engineering deals with mathematical modelling of physiological (cardiac, lung ventilation, glucose regulation) systems and formulation of indices for medical assessment (such as cardiac contractility, lung disease status, and diabetes risk). Finally, Hospital management science and technology involves the application of both biomedical engineering and industrial engineering for cost-effective operation of a hospital.

How to reference

In order to correctly reference this scholarly work, feel free to copy and paste the following:

Dhanjoo N. Ghista, U. Rajendra Acharya, Kamlakar D. Desai, Sarma Dittakavi, Adejuwon A. Adeneye and Loh Kah Meng (2012). Diabetes Mechanisms, Detection and Complications Monitoring, Biomedical Science, Engineering and Technology, Prof. Dhanjoo N. Ghista (Ed.), ISBN: 978-953-307-471-9, InTech, Available from: http://www.intechopen.com/books/biomedical-science-engineering-and-technology/diabetes-mechanisms-detection-and-complications-monitoring

INTECH
open science | open minds

InTech Europe
University Campus STeP Ri
Slavka Krautzeka 83/A
51000 Rijeka, Croatia
Phone: +385 (51) 770 447
Fax: +385 (51) 686 166

InTech China
Unit 405, Office Block, Hotel Equatorial Shanghai
No.65, Yan An Road (West), Shanghai, 200040, China
中国上海市延安西路65号上海国际贵都大饭店办公楼405单元
Phone: +86-21-62489820
Fax: +86-21-62489821

www.intechopen.com

IntechOpen

IntechOpen